お茶の水女子大学自然科学報告　第71巻　特別号
Natural Science Report, Ochanomizu University, Vol. 71, Special Issue（2020）

Construction of Self-Assembled Monolayer of 4-Aminothiophenol (4-ATP) on Au(100) Substrate

Mami Takahari and Toshihiro Kondo*

Division of Chemistry, Graduate School of Humanities and Sciences, Ochanomizu University, 2-1-1, Ohtsuka, Bunkyo-ku, Tokyo 112-8610, Japan
* kondo.toshihiro2@ocha.ac.jp

(Received May 1, 2020)

Abstract: In order to play a role of a linker between a functional molecular layer and the electrode substrate, the method to prepare the self-assembled monolayer of 4-aminothiophenol (4-ATP), with the terminal amino group which can connect an anion, on Au(100) was investigated. The adsorption amount, orientation, and stability were examined based on the results of the electrochemical reductive desorption measurements.

1. Introduction

In the electrodes modified with the molecular layers with various functionalities, in order to efficiently take place electron transfer between the electrode and the functional molecular layer, it is of great importance to control the structure of the linker layer that connects the molecular layer and the single-crystal electrode surface at the molecular dimension. Self-assembled monolayers (SAMs) of alkylthiols on gold have been extensively studied because of their high density, regular orientation, and high stability, and have been applied to various fields, such as sensors, corrosion inhibition, wetting control, and molecular electronic devices, because the alkylthiol SAMs can connect the gold substrate surface and the molecular layers with various functionalities [1-8].

Since many functional molecules have a 4-fold symmetry crystal structure, a single-crystal Au substrate, of which surface atomic arrangement has 4-fold symmetry, like a Au(100) single-crystal substrate is desirable. Because of the ease of the preparation, however, there are most of the studies on the SAMs on Au(111) , which has 3-fold symmetry, and few studies on the SAM on Au(100) [3,10].

On the other hand, in order to construct a functional molecular layer containing anions, a cation terminated SAM is required. As one of them, an amino-terminated 4-aminothiophenol (4-ATP) SAM has been well-studied [11-25]. However, the role of the 4-ATP SAM is to simply adsorb the deposit on the polycrystalline Au substrate [11-19] or to control the orientation on Au(111) with 3-fold symmetry [20-25]. There is no discussion about the dependence of the preparation method on the structure and orientation of the 4-ATP SAM formed on Au(100) with 4-fold symmetry.

Here, two kinds of solvents, ethanol which is a polar solvent and hexane which is a non-polar solvent were employed as a solvent for the 4-ATP SAM preparation and the adsorption amount, orientation, and stability of 4-ATP SAMs, which were prepared by immersing the Au(100) substrate in the 4-ATP solutions for various periods, on Au(100) were discussed based on the results of the electrochemical reductive desorption measurements [26].

2. Material and Methods

Materials.

Au(100) single-crystal disk (diameter: 10 mm, thickness: 5 mm) was purchased from SPL and used after the pretreatments [27,28]. 4-ATP (97.0%) was

purchased from Wako Pure Chemicals, reagent grade ethanol, hexane, H_2SO_4 were from Kanto Chemicals, and semiconductor grade KOH was from Aldrich. All the chemicals were used without any further purification. Platinum wire (99.999%, diameter: 0.5 mm) was purchased from Nilaco Co. Water was purified using a Milli-Q system (Sartorius, arium®pro UV/DI). Ultrapure Ar gas (99.9995%) and pure N_2 gas (99.99%) were purchased from Kotobuki Sangyo.

Sample Preparation

Prior to each sample preparation, the Au(100) single-crystal disk substrate was flame-annealed using a Bunsen burner and was quenched with an ultra-pure water. Then, the Au(100) disk was immersed in ethanol or hexane solution containing 1 mM 4-ATP at room temperature (RT) for several periods from 10 min. to 5 hours. The substrate was then rinsed with ethanol or hexane, respectively, and was dried with N_2 blowing.

Measurements

Electrochemical measurements were carried out in an Ar-saturated 50 mM H_2SO_4 solution and in an Ar-saturated 0.1 M KOH solution for checking the real surface area of the Au(100) electrode [28] and for the evaluation of the adsorbed amount of 4-ATP molecules on Au(100) [26], respectively, using the conventional three-electrode cell with the Hg/Hg_2SO_4 electrode (MSE) and Ag/AgCl electrode, respectively, as an reference electrode and with a Pt wire as a counter electrode.

X-ray photoelectron spectroscopy (XPS) measurements were performed with the XPS system (Thermo Fisher Scientific, K-Alpha) under ambient pressure less than 10^{-4} Pa using AlKα x-ray (1486.6 eV) as an x-ray source.

3. Results

Figure 1 shows the cyclic voltammogram (CV) of the Au(100) single-crystal electrode, measured in the deaerated 50 mM H_2SO_4 solution just after Au(100) disk was flame-annealed and quenched. Two typical oxidation peaks at +0.64 V (vs. MSE) and +0.68 V for Au(100) showed that most of the surface of the present Au disk is the regulated Au(100) plane, but the relatively small oxidation peak was also observed at +0.85 V, indicating that a part of the surface is the Au(111) plane [28].

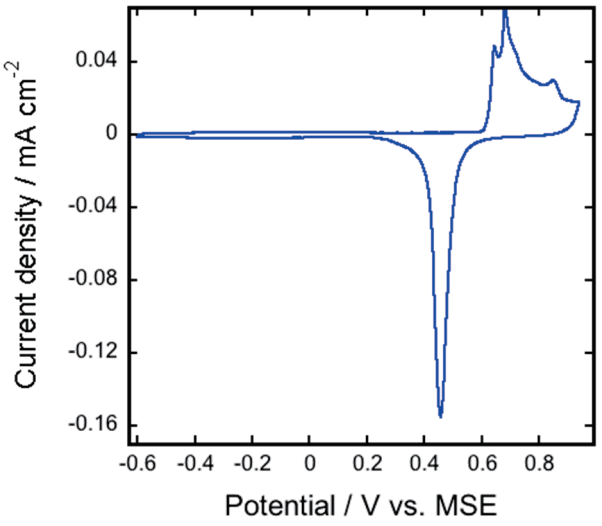

Figure 1. The CV of the Au(100) electrode, measured in the Ar-saturated 50 mM H_2SO_4 solution with a scan rate of 20 mV s^{-1}.

Based on the charge of the cathodic peak, which is due to the reduction of the outermost surface Au oxide layer, observed at +0.45 V, we can obtain the surface area to be 0.877 cm^2 (roughness factor: 1.12) [28], showing that most of the surface of the present Au(100) disk is atomically flat.

Using this Au(100) disk electrode, the 4-ATP SAMs were constructed by dipping the disk substrate into the 1 mM 4-ATP in ethanol or hexane for several dipping periods. Figure 2 shows the linear sweep voltammograms (LSVs) of the Au(100) modified with the 4-ATP SAM, prepared from the ethanol solution (Fig. 2(a)) and hexane solution (Fig. 2(b)) by the several dipping periods, measured in the deaerated 0.1 M KOH solution when the potential scan started at 0 V to the negative direction. In both the LSVs shown in Figs. 2(a) and 2(b), one dominant cathodic peak was

observed around -0.9 V (vs. Ag/AgCl), which is due to the reductive desorption of the 4-ATP SAM from the Au(100) surface [26].

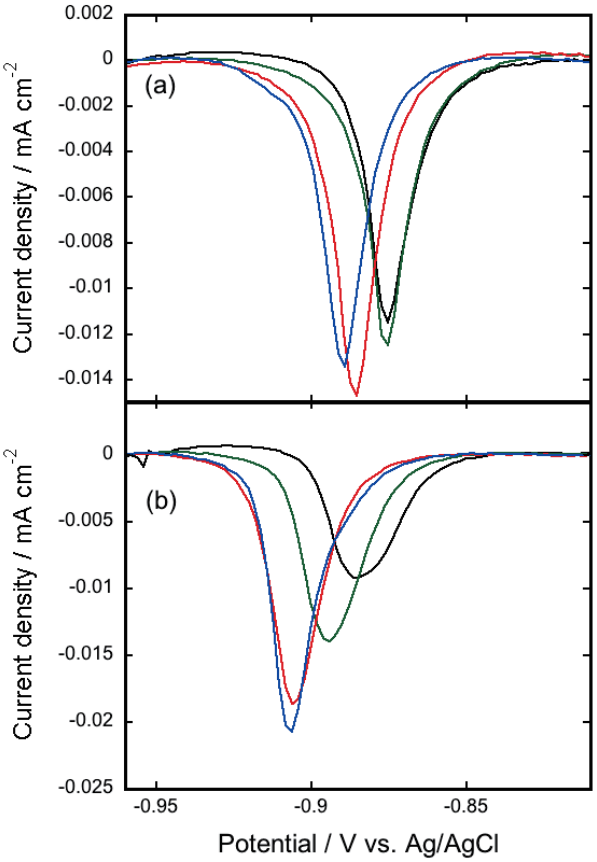

Figure 2. LSVs of the Au(100) electrodes modified with the 4-ATP SAMs, which prepared (a) from the ethanol solution and (b) from the hexane solution, measured in the Ar-saturated 0.1 M KOH solution with a scan rate of 20 mV s^{-1}. Dipping periods were 10 min (black), 1 hour (green), 3 hours (red), and 5 hours (blue).

Based on the literature [1,26], the alkylthiol SAM formed on gold (R-S / Au) is reductively desorbed from the gold surface with an electron (e^-) as follows;

$$R\text{-}S / Au + e^- \rightarrow R\text{-}S^- + Au \quad (1)$$

where $R\text{-}S^-$ represents alkylthiolate anion. Therefore, it is possible to obtain the adsorption amount from the integrated charge (nmol cm^{-2}) of the reductive peak, the stability of the SAM from the peak potential (V), and the orientation of the SAM from the full width at half maximum (FWHM) (mV) of the corresponding peak [26].

Figure 3 shows the dipping period dependences of the adsorbed amount, peak potential, and FWHM of the cathodic peak due to the reductive desorption of the 4-ATP SAM in Fig. 2.

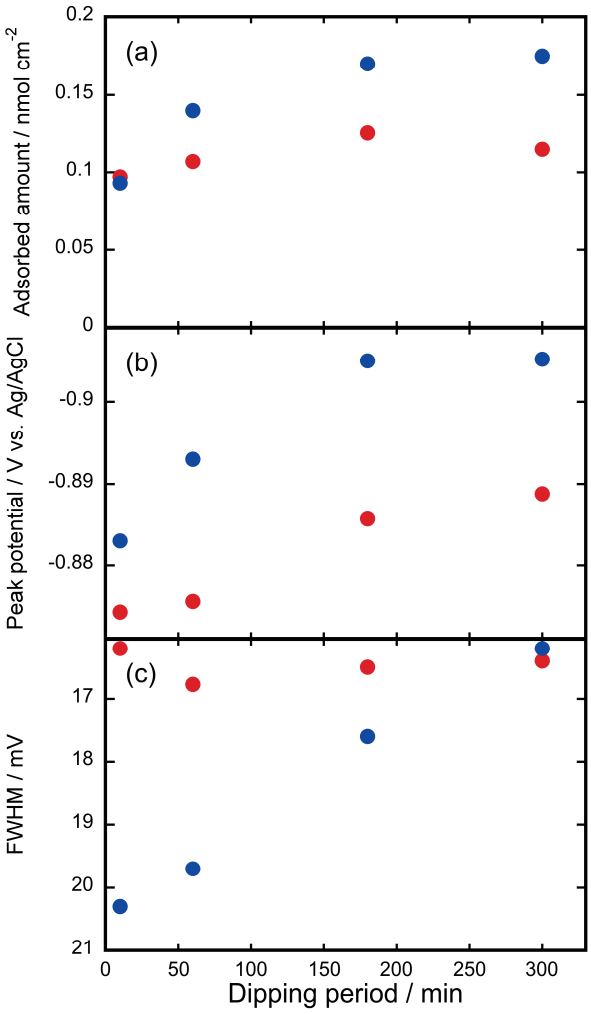

Figure 3. Dipping period dependences of (a) the adsorbed amount (nmol cm^{-2}), (b) peak potential (V vs. Ag/AgCl), and (c) FWHM values (mV) of the reductive current peak observed from the LSVs in Fig. 2. Data points, from which the 4-ATP SAM was prepared from the ethanol and hexane solutions, represent the red and blue, respectively, circles.

In the both dipping solvent cases, the adsorbed amount increased, the peak potential negatively shifted, and the FWHM value became smaller, with the dipping period, indicating that the longer the dipping period, the better the SAM formed. In both the 4-ATP SAMs prepared from the ethanol and hexane solutions, values of each factor were saturated by the dipping for 5 hours. Comparing 4-ATP SAM prepared from the ethanol solution with that prepared from the hexane solution, that prepared from the hexane solution showed better values for all factors. This is probably because 4-ATP is not protonated in hexane, which is a non-polar solvent, and then a uniform intermolecular interaction take place during SAM formation. On the other hand, in ethanol, which is a polar solvent, 4-ATP is a little protonated and then, the intermolecular interaction at each site of the molecule differ during the formation of the 4-ATP SAM, which may result in the formation of the relatively low-quality SAM. When the 4-ATP SAM was constructed on Au(111) using the same ethanol solution, the similar low-quality 4-ATP SAM is formed [20]. Therefore, it can be concluded that the highest quality 4-ATP SAM can be constructed by dipping the Au(100) single-crystal disk in the 1 mM hexane solution for more than 5 hours at RT. Although there is also report that high-quality 4-ATP SAM on Au(111) was prepared by dipping the Au substrate into the ethanol solution with much lower concentration of 4-ATP for more than 1 day [25], we only compared solvents at the same 4-ATP concentration.

In order to further characterize the 4-ATP SAM, the XP spectra of the 4-ATP SAM modified Au(100) substrate, which were prepared by dipping the Au(100) disk into the hexane solution containing 1 mM 4-ATP for 5 hours at RT, were measured. Figures 4(a) and 4(b) show the XP spectra of the 4-ATP SAM fully modified Au(100) disks in the S2p and the N1s regions, respectively.

In the S2p region (Fig. 4(a)), three different kinds of S species, which were labelled S_A, S_B, and S_C, as shown in red, blue, and green lines, respectively, in Fig. 4(a) were observed as a result of the peak fitting. S_A and S_B species were assigned to a S atom covalently bonded to gold [29-35] and to a S atom forming the disulfide [36-39], respectively. Therefore, it was found that not only 4-ATP forming a direct covalent bond with gold atoms but also 4-ATP forming a disulfide bond and then physorbed as a dimer are present on the Au(100) surface. S_C species was identified as a S atom forming oxide [39-41], but we cannot clear when this species formed.

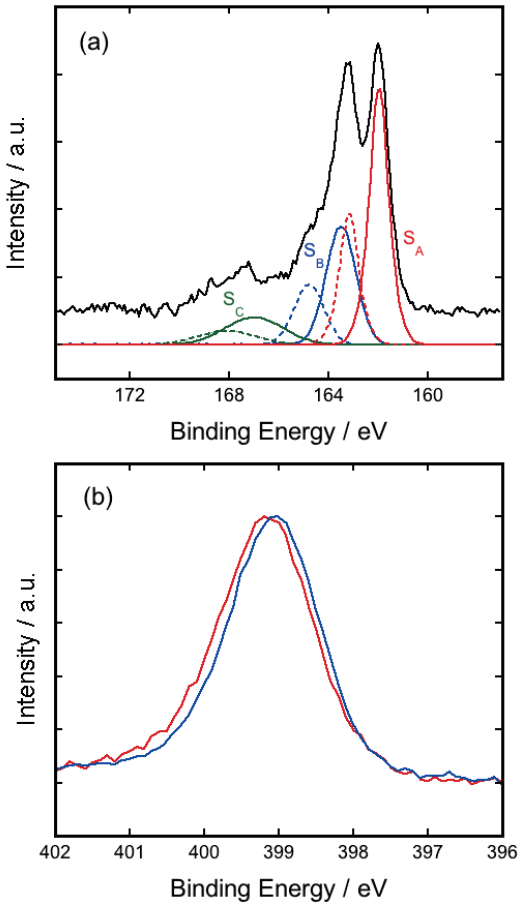

Figure 4. (a) XP spectrum of the 4-ATP SAM fully modified Au(100) substrate in the S2p region. The raw spectrum represents black and each separated spectrum is shown in red, blue, and green. The solid and dotted lines correspond to 3/2 and 1/2 of the S2p region, respectively. (b) XP spectra of the 4-ATP SAM formed from ethanol (red) and hexane (blue) solutions in N1s region.

In the 4-ATP SAM formed from both solvents, only one peak was observed around 399 eV in the N1s region (Fig. 4(b)). As clearly seen in Fig. 4(b), the peak in the case of forming from ethanol (399.2 eV) was observed slightly higher than that in the case of forming from hexane (399.0 eV). When the amino group is protonated, the N1s peak is shifted to higher energy. Actually, the N1s peak was observed at relatively high binding energy when the 4-ATP SAM was constructed on Au(111) using the same ethanol solution [20]. However, it is considered in the present study that the peak was not shifted, because the XPS measurement was performed under ultra-high vacuum (UHV).

4. Conclusion

As a result of forming 4-ATP SAM on Au(100) by using ethanol as a polar solvent and hexane as a non-polar solvent, it was found that all the density, stability, and orientation of the 4-ATP SAM preparing from the hexane solution are much higher than those from ethanol solution. As a factor of this, the XP spectra suggested that the amino group was not protonated in the non-polar solvent.

References

1. Ulman, A. *An Introduction to Ultrathin Organic Films from Langmuir-Blodgett to Self-Assembly,* Academic Press, New York, **1991**.
2. Finklea, O. in *Electroanalytical Chemistry*, edited by Bard A. J. and Rubinstein, I., Marcel Dekker, New York, **1996**, Vol. 19, p. 109.
3. Kondo, T., Yamada, R., Uosaki, K. Self-Assembled Monolayer (SAM) in *Organized Organic Ultrathin Films – Fundamentals and Applications*, edited by Ariga, K., Wiley-VCH, Wenheim, Chap. 2, 7-42 (2012).
4. Uosaki, K., Kondo, T., Zhang, X.-Q., Yanagida, M. Very Efficient Visible-Light-Induced Uphill Electron Transfer at a Self-Assembled Monolayer with a Porphyrin-Ferrocene-Thiol Linked Molecule. *J. Am. Chem. Soc.*, **119**, 8367-8368 (1997). https://doi.org/10.1021/ja970945p
5. Kondo, T., Horiuchi, S., Yagi, I., Ye, S., Uosaki, K. Electrochemical Control of the Second Harmonic Generation Property of Self-Assembled Monolayers Containing a *trans*-Ferrocenyl-Nitrophenyl Ethylene Group on Gold. *J. Am. Chem. Soc.*, **121**, 391-398 (1999). https://doi.org/10.1021/ja982007a
6. Kondo, T., Kanai, T., Uosaki, K. Control of the Charge-Transfer Rate at a Gold Electrode Modified with a Self-Assembled Monolayer Containing Ferrocene and Azobenzene by Electro- and Photochemical Structural Conversion of Cis and Trans Forms of the Azobenzene Moiety. *Langmuir*, **17**, 6317-6324 (2001). https://doi.org/10.1021/la0108914
7. Kondo, T., Sato, S., Construction of Highly Oriented Self-Assembled Monolayer of Alkyldithiol with Ferrocene on Gold(111) Using Underpotentially Deposited Lead Submonolayer as a Template. *Chem. Lett.*, **36**, 1216-1217 (2007). https://doi.org/10.1246/cl.2007.1216
8. Umezawa, N., Tsurunari, M., Kondo, T. Electrochemical Atrazine Detection Using Au(111) Electrode Modified with Self-Assembled Monolayer of Mercaptoquinone. *Chem. Lett.*, **38**, 766-767 (2009). https://doi.org/10.1246/cl.2009.766
9. Aoki, N., Sato, K., Hasegawa, K., Sano, S., Kageyama, M. Umezawa, N., Kondo, T. Self-Assembly Process of Flatly Adsorbed Porphyrin Self-Assembled Monolayer on a Au(111) Surface Studied by ex situ Scanning Tunneling Microscopy and Electrochemical Reductive Desorption Measurements. *Electrochemistry*, **82**, 385-390 (2014). https://doi.org/10.5796/electrochemistry.82.385
10. Vericat, C., Vela, M. E., Corthey, G., Pensa, E., Cortés, E., Fonticelli, M. H., Ibañez, F., Benitez, G. E., Carro, P., Salvarezza, R. C. Self-assembled

monolayers of thiolates on metals: a review article on sulfur-metal chemistry and surface structures. *RSC Adv.*, **4**, 27730-27754 (2014). https://doi.org/10.1039/C4RA04659E

11. Kajiya, Y., Okamoto, T., Yoneyama, H., Glucose sensitivity of thiol-modified gold electrodes having immobilized glucose oxidase and 2-aminoethylferrocene. *Chem. Lett.*, **12**, 2107-2110 (1993). https://doi.org/10.1246/cl.1993.2107
12. Cho, S. H., Kim, D., Park, S.-M. Electrochemistry of conductive polymers: 41. Effects of self-assembled monolayers of aminothiophenols on polyaniline films. *Electrochim. Acta*, **53**, 3820-3827 (2008). https://doi.org/10.1016/j.electacta.2007.08.076
13. Mezour, M. A., Cornut, R., Hussien, E. M., Morin, M., Mauzeroll, J. Detection of Hydrogen Peroxide Produced during the Oxygen Reduction Reaction at Self-Assembled Thiol-Porphyrin Monolayers on Gold using SECM and Nanoelectrodes. *Langmuir*, **26**, 13000-13006 (2010). https://doi.org/10.1021/la100444n
14. Scavetta, E., Solito, A. G., Demelas, M., Cosseddu, P., Bonfiglio, A. Electrochemical characterization of self assembled monolayers on flexible electrodes. *Electrochim. Acta*, **65**, 159-164 (2012). https://doi.org/10.1016/j.electacta.2012.01.033
15. Demissie, A. T., Haugstad, G., Frisbie, C. D. Growth of Thin, Anisotropic, π-Conjugated Molecular Films by Stepwise "Click" Assembly of Molecular Building Blocks: Characterizing Reaction Yield, Surface Coverage, and Film Thickness versus Addition Step Number. *J. Am. Chem. Soc.*, **137**, 8819-8828 (2015). https://doi.org/10.1021/jacs.5b04512
16. Silva, C. P., Santander-Nelli, M., Vera-Oyarce, C., Silva, J. F., Gomez, A., Munoz, L. A., Zagal, J. H., Gullpi, M., Pavez, J. Polyaniline nanostructure electrode: morphological control by a hybrid template. *J. Solid State Electrochem.*, **20**, 1175-1180 (2016). https://doi.org/10.1007/s10008-015-2944-2
17. Bourone, S. D., Kaulen, C., Homberger, M., Simon, U. Direct Self-Assembly and Infrared Reflection Absorption Spectroscopy Analysis of Amphiphilic and Zwitterionic Janus Gold Nanoparticles. *Langmuir*, **32**, 954-962 (2016). https://doi.org/10.1021/acs.langmuir.5b03897
18. Sapountzi, E., Braiek, M., Vocanson, F., Chateaux, J.-F., Jaffrezic-Renault, N., Lagarde, F. Gold nanoparticles assembly on electrospun poly(vinyl alcohol)/poly(ethyleneimine)/glucose oxidase nanofibers for ultrasensitive electrochemical glucose biosensing. *Sensors Actuators, B: Chemical*, **238**, 392-401 (2017). https://doi.org/10.1016/j.snb.2016.07.062
19. Sepulveda, D., Aroca, M. A., Varela, A., Del Portillo, P., Osma, J. F. Bioelectrochemical detection of Mycobacterium tuberculosis ESAT-6 in an antibody-based biomicrosystem. *Sensors*, **17**, 2178/1-2178/14 (2017). https://doi.org/10.3390/s17102178
20. Arima, V., Matino, F., Thompson, J.; Cingolani, R., Rinaldi, R., Blyth, R. I. R. Ex-situ prepared films of 4-aminothiophenol on Au(111): photoemission, NEXAFS and STM measurements. *Surf. Sci.*, **580**, 63-70 (2005). https://doi.org/10.1016/j.susc.2005.02.009
21. Ponce, I., Silva, J. F., Onate, Ruben, Rezende, M. C., Paez, M. A., Pavez, J., Zagal, J. H. Enhanced catalytic activity of Fe phthalocyanines linked to Au(111) via conjugated self-assembled monolayers of aromatic thiols for O_2 reduction. *Electrochem. Commun.*, **13**, 1182-1185 (2011). https://doi.org/10.1016/j.elecom.2011.08.050
22. Ponce, I., Silva, J. F., Onate, R., Miranda-Rojas, S., Munoz-Castro, A., Arratia-Perez, R., Mendizabal, F., Zagal, J. H. Theoretical and Experimental Study of Bonding and Optical Properties of Self-Assembly Metallophthalocyanines Complexes on a Gold Surface. A Survey of the Substrate-Surface

Interaction. *J. Phys. Chem. C*, **115**, 23512-23518 (2011).
https://doi.org/10.1021/jp208734f

23. Nishino, T., Kanata, S., Hirata, C. Immobilization of carbon nanotubes on Au(111) via self-assembled monolayers. *Chem. Lett.*, **40**, 1217-1219 (2011).
https://doi.org/10.1246/cl.2011.1217
24. Ponce, I., Silva, J. F., Onate, R., Rezende, M. C., Paez, M. A., Zagal, J. H., Pavez, J., Mendizabal, F., Miranda-Rojas, S., Munoz-Castro, A., Enhancement of the Catalytic Activity of Fe Phthalocyanine for the Reduction of O_2 Anchored to Au(111) via Conjugated Self-Assembled Monolayers of Aromatic Thiols As Compared to Cu Phthalocyanine. *J. Phys. Chem. C*, **116**, 15329-15341 (2012).
https://doi.org/10.1021/jp301093q
25. Silva, J. F., Pavez, J., Silva, C. P., Zagal, J. H. Electrocatalytic activity of modified gold electrodes based on self-assembled monolayers of 4-mercaptopyridine and 4-aminothiophenol on Au(111) surfaces chemically functionalized with substituted and unsubstituted iron phthalocyanines. *Electrochim. Acta*, **114**, 7-13 (2013).
https://doi.org/10.1016/j.electacta.2013.10.017
26. Widrig, C. A., Chung, C., Porter, M. D. The electrochemical desorption of n-alkanethiol monolayers from polycrystalline Au and Ag electrodes. *J. Electroanal. Chem.,* **310**, 335-359 (1991).
https://doi.org/10.1016/0022-0728(91)85271-P
27. Ye, S., Ishibashi, C., Uosaki, K. Anisotropic Dissolution of an Au(111) Electrode in Perchloric Acid Solution Containing Chloride Anion Investigated by in Situ STM – The Important Role of Adsorbed Chloride Anion. *Langmuir*, **15**, 807-812 (1999).
https://doi.org/10.1021/la980812x
28. Kondo, T., Morita, J., Hanaoka, K., Takakusagi, S., Tamura, K., Takahasi, M., Mizuki, J., Uosaki, K. Structure of Au(111) and Au(100) Single-Crystal Electrode Surfaces at Various Potentials in Sulfuric Acid Solution Determined by In Situ Surface X-ray Scattering. *J. Phys. Chem. C*, **111**, 13197-13204 (2007).
https://doi.org/10.1021/jp072601j
29. Zubavichus, Y., Zharnikov, M., Grunze, M. X-ray Photoelectron Spectroscopy and Near-Edge X-ray Absorption Fine Structure Study of Water Adsorption on Pyridine-Terminated Thiolate Self-Assembled Monolayers. *Langmuir,* **20**, 11022-11029 (2004).
https://doi.org/10.1021/la047980b
30. Gao, D., Scholz, F., Nothofer, H. G., Wrochem, F. Fabrication of Asymmetric Molecular Junctions by Oriented Assembly of Dithiocarbamate Rectifiers. *J. Am. Chem. Soc.,* **133**, 5921-5930 (2011).
https://doi.org/10.1021/ja110244j
31. Castner, D. G. X-ray Photoelectron Spectroscopy Sulfur 2p Study of Organic Thiol and Disulfide Binding Interactions with Gold Surfaces. *Langmuir,* **12**, 5083-5086 (1996).
https://doi.org/10.1021/la960465w
32. Ahn, H., Whitten, J. E. Potassium deposition on a thiophene-terminated alkanethiol monolayer. *J. Electron. Spectrosc. Relat. Phenom.,* **172**, 107-113 (2009).
https://doi.org/10.1016/j.elspec.2009.03.015
33. Yang, Y. W., Fan, L. J. High-Resolution XPS Study of Decanethiol on Au(111): Single Sulfur-Gold Bonding Interaction. *Langmuir,* **18**, 1157-1164 (2002).
https://doi.org/10.1021/la010591m
34. Shimazu, K., Takechi, M., Fujii, H., Suzuki, M., Saiki, H., Yoshimura, T., Uosaki, K. Formation and characterization of thiol-derivatized zinc(Ⅱ) porphyrin monolayers on gold. *Thin Solid Films,* **273**, 250-253 (1996).
https://doi.org/10.1016/0040-6090(95)06790-6
35. Gonella, G., Cavalleri, O., Terreni, S., Cvetko, D., Floreano, L., Mortante, A., Canepa, M., Rolandi, R. High resolution X-ray photoelectron spectroscopy

of 3-mercaptopropionic acid self-assembled films. *Surf. Sci.,* **566**, 638-643 (2004).
https://doi.org/10.1016/j.susc.2004.05.125

36. Ishida, T., Choi, N. High-Resolution X-ray Photoelectron Spectra of Organosulfur Monolayers on Au(111): S(2p) Spectral Dependence on Molecular Species. *Langmuir,* **15**, 6799-6806 (1999).
https://doi.org/10.1021/la9810307
37. Whelan, C. M., Smyth, M. R., Barnes, C. J., Brown, N. M. D., Anderson, C. A. An XPS study of heterocyclic thiol self-assembly on Au(111). *Appl. Surf. Sci.,* **134**, 144-158 (1998).
https://doi.org/10.1016/S0169-4332(98)00204-9
38. Jameson, D. L., Xie, C-L., Hendrickson, D. N., Potenza, J. A., Schugar, H. J. Molecular structure and magnetic properties of a novel Fe(III) tetranuclear complex containing oxo, alkoxo, and carbonate bridges. *J. Am. Chem. Soc.,* **109**, 740-746 (1987).
https://doi.org/10.1021/ja00237a018
39. Bain, C. D., Biebuyck, H. A., Whitesides, G. M. Comparison of Self-Assembled Monolayers on Gold: Coadsorption of Thiols and Disulfides. *Langmuir,* **5**, 723-727 (1989).
https://doi.org/10.1021/la00087a027
40. Genorio, B., He, T., Meden, A., Polanc, S., Jamnik, J., Tour, J. M. Synthesis and Self-Assembly of Thio Derivatives of Calix[4]arene on Noble Metal Surfaces. *Langmuir,* **24**, 11523-11532 (2008).
https://doi.org/10.1021/la802197u
41. Medard, C., Morin, M. Chemisorption of aromatic thiols onto a glassy carbon surface. *J. Electoranal. Chem.,* **632**, 120-126 (2009).
https://doi.org/10.1016/j.jelechem.2009.04.005

Acknowledgement

This work was partially supported by Grants-in-Aids for Scientific Research (C) (KAKENHI, No. 26410008) from the Ministry of Education, Culture, Sports, Science, and Technology (MEXT), Japan.